Structure and Aggregation Number of a Lyotropic Liquid Crystal: A Fluorescence Quenching and Molecular Dynamics Study

ARTICLE *in* LANGMUIR · AUGUST 2004

Impact Factor: 4.46 · DOI: 10.1021/la049801w · Source: PubMed

8 AUTHORS, INCLUDING:

Rodrigo Montecinos
Pontifical Catholic University of Chile
15 PUBLICATIONS **51** CITATIONS
SEE PROFILE

Andres Olea
Autonomous University of Chile
70 PUBLICATIONS **959** CITATIONS
SEE PROFILE

Ramiro Araya-Maturana
Universidad de Talca
92 PUBLICATIONS **476** CITATIONS
SEE PROFILE

Structure and Aggregation Number of a Lyotropic Liquid Crystal: A Fluorescence Quenching and Molecular Dynamics Study

R. Montecinos,[†] H. Ahumada,[†] R. Martínez,[†] F. A. Olea,[†] R. Araya-Maturana,[‡] M. P. Aliste,[§] D. P. Tieleman,[||] and B. E. Weiss-López*,[†]

Departamento de Química, Facultad de Ciencias, Universidad de Chile, Casilla 653, Santiago, Chile, Departamento de Química Orgánica y Fisicoquímica, Facultad de Ciencias Químicas y Farmacéuticas, Universidad de Chile, Casilla 233, Santiago 1, Chile, School of Biology, Georgia Institute of Technology, 310 Ferst Drive, Atlanta, Georgia 30332-0230, and Department Biological Sciences, University of Calgary, 2500 University Drive 1 NW, Calgary, Alberta T2N 1N4, Canada

The structure and aggregation number of a discotic lyotropic liquid crystal, prepared from tetradecyltrimethylammonium chloride (TDTMACl)/decanol (DeOH)/NaCl/H_2O, have been examined using fluorescence quenching of pyrene by hexadecylpyridinium chloride and molecular dynamics (MD). The fluorescence method gives an aggregation number of 258 ± 25 units (DeOH + TDTMACl). From the MD simulation, a lower limit for the aggregate dimension of 130 units of DeOH + TDTMACl is predicted. A stable oblate aggregate of 240 units was studied in detail. A strong polarization between the ammonium headgroups and chloride ions is observed from the calculated trajectory. DeOH headgroups are located, on average, 0.3 nm more to the interior of the aggregate than the TDTMACl headgroup and contribute to widening the interface by forming H-bonds with water. The radial distribution function of the ammonium headgroup shows that there are 16 water molecules in the first solvation sphere. The diagonal elements of the order parameter tensor of the tail atoms of both surfactants indicate that the interior of the micelle preserves about the same degree of order as at the interface, up to the last three atoms of the aliphatic chain, where the order starts to decrease.

Introduction

Nematic lyotropic liquid crystals have been recently rediscovered as a low-order orienting medium in chemical and biochemical applications.[1−4] These materials, first observed by Lawson and Flautt,[5] are composed of aggregates of surfactant molecules dissolved in water, usually with some amount of alcohol and salt added. Two different types of uniaxial surfactant aggregates with different magnetic properties have been identified: one with positive diamagnetic anisotropy, N_c, composed of cylindrical micelles with *prolate* average symmetry, and the other with negative diamagnetic anisotropy, N_D, which corresponds to disklike bilayer micelles of *oblate* average symmetry.[6−8] More recently, the morphology of three different lyotropic liquid crystals employed in biological NMR was studied by measuring the anisotropic behavior of the translational diffusion coefficients. The studied systems were aqueous solutions of the following mixtures: (a) pentakis(ethylene glycol) monodecyl ether/hexanol; (b) cetylpyridinium bromide/hexanol and dimyristoylphosphatidylcholine/dicyclohexylphosphatidylcholine.This study corroborates the lamellar nature of the aggregates.[9] The use of lyotropic liquid crystalline media with low order and appropriate solubility properties as a medium to align particular substrates has improved the accuracy of structure determinations of biologically interesting macromolecules and in the study of intermolecular interactions.[10−13] Here we study the structure and aggregation number of a discotic lyotropic liquid crystal prepared by dissolving tetradecyltrimethylammonium chloride (TDTMACl), 1-decanol (DeOH), and NaCl in water. As far as we know it is the first time a study like this is attempted in a four-component discotic nematic lyotropic liquid crystal. However, the aggregation number of the binary system composed of cesium pentadecafluorooctanoate in water has been experimentally determined using NMR.[14] In this paper we have used static fluorescence quenching of pyrene by hexadecylpyridinium chloride (HDPYCl)[15,16] and molecular dynamics[17] simulation.

[†] Departamento de Química, Universidad de Chile.
[‡] Departamento de Química Orgánica y Fisicoquímica, Universidad de Chile.
[§] School of Biology, Georgia Institute of Technology.
[||] Department Biological Sciences, University of Calgary.

(1) Weise, C. F.; Weisshaar, J. C. *J. Phys. Chem. B* **2003**, *107*, 6552−6564.
(2) Bertini, I.; Castellani, F.; Luchinat, C.; Martini, G.; Parigi, G.; Ristori, S. *J. Phys. Chem. B* **2000**, *104*, 10653−10658.
(3) Tan, C. B.; Fung, B. M.; Cho, G. J. *J. Am. Chem. Soc.* **2002,** *124*, 11827−11832.
(4) Khetrapal, C. L. *J. Indian Chem. Soc.* **2001**, *78*, 112−114.
(5) Lawson, K. D.; Flautt, T. J. *J. Am. Chem. Soc.* **1967**, *89*, 5489−5491.
(6) Amaral, L. Q.; Pimentel, C. A.; Tavares, M. R.; Vanin, J. A. *J. Chem. Phys.* **1979**, *45*, 2940−2945.
(7) Charvolin, J.; Levelut, A. M.; Samulski, E. T. *J. Phys. Lett.* **1979**, *40*, 587−592.
(8) Radley, K.; Reeves, L.; Tracey, A. S. *J. Phys. Chem.* **1976**, *80*, 174−182.
(9) Gaemers, S.; Bax, A. *J. Am. Chem. Soc.* **2001**, *123*, 12343−12352.
(10) Tjandra, N.; Omichinski, J. G.; Gronenborn, A. M.; Clore, G. M.; Bax, A. *Nat. Struct. Biol.* **1997**, *4*, 732−738.
(11) Ottiger, M.; Bax, A. *J. Biomol. NMR* **1999**, *13*, 187−191.
(12) Olejniczak, E. T.; Meadows, R. P.; Wang, H.; Cai, M. L.; Nettesheim, D. G.; Fesik, S. W. *J. Am. Chem. Soc.* **1999**, *121*, 9249−9250.
(13) Clore, G. M. *Proc. Natl. Acad. Sci. U.S.A.* **2000**, *97*, 9021−9025.
(14) Johannesson, H.; Furó, I.; Halle, B. *Phys. Rev. E* **1996**, *53*, 4904−4917.
(15) Alargova, R. G.; Kochijashky, I. I.; Sierra, M. L.; Zana, R. *Langmuir* **1998**, *14*, 5412−5418.
(16) Turro, N. J.; Yekta, A. *J. Am. Chem. Soc.* **1978**, *100*, 5951−5952.

Materials and Methods

Mesophase and Sample Preparation. TDTMACl was prepared from commercially available TDTMABr, using a previously described methodology.[18] The purity of the product was tested by conductometric measurement of the critical micelle concentration (cmc).[19] The obtained value, 0.006 M, is in good agreement with a previously reported cmc, 0.004 M.[20] The liquid crystal solution was prepared by dissolving 5.46 g of TDTMACl, 1.71 g of NaCl, and 1.38 mL of DeOH in 15 mL of H_2O. One sample of TDTMABr and one of TDTMACl, both with the same molar composition, were prepared using 10% DeOH-α-d_2 and H_2O with 0.1% D_2O for ^2H NMR quadrupole splitting measurements. DeOH-α-d_2 was prepared by reduction of the ethyl ester of decanoic acid with $LiAlD_4$. The mesophase with bromide instead of chloride as counterion had been prepared before,[21] and the composition employed in this work (with chloride) is very similar. Polarized light microscopy and ^2H NMR quadrupole splittings were employed to characterize the mesophase. The textures observed in TDTMACl under the polarized light microscope (Leica DMPL) correspond to typical lamellar material.[22] Residual quadrupole splittings of HDO and decanol-α-d_2 were measured at 64 MHz with a Bruker Avance 400 NMR spectrometer. The ^2H NMR spectrum confirms the nematic nature of the mesophase. The observed deuterium quadrupole splittings in the chloride mesophase were 13.2 kHz for DeOH-α-d_2 and 7 Hz for HDO, much smaller than the splittings observed in the bromide mesophase, 19.9 kHz and 34 Hz, respectively. The measured quadrupole splittings are directly related to the order parameter of the principal axis of the electric field gradient, approximately the C−D bond, with respect to the magnetic field direction. The order parameter describes the spread of the angular distribution of this bond with respect to the field direction. It can have values from −0.5, for a C−D axis oriented perpendicular to the magnetic field, to +1, for an axis parallel to the field. The value zero can arise only from an axis at the magic angle or a freely rotating axis. The differences observed between TDTMACl and TDTMABr mesophases can be explained on the basis of two effects: (1) the characteristics of the counterions and the added salt and/or (2) the possibility that the TDTMABr aggregate is bigger than the TDTMACl aggregate. Since chloride is smaller than bromide, it generates a larger electrostatic potential and prefers the aqueous environment when compared to bromide, which is bigger and probably located closer to the interface, leading to partial neutralization of the ammonium headgroups and order. These two effects should be responsible for the observed differences in quadrupole splittings. Experiments to determine the aggregation number of TDTMABr are currently being carried out.

Fluorescence Quenching. A series of steady-state fluorescence spectra of pyrene quenched by HDPYCl allows an estimate of the micellar aggregation number.[15,16] Eight microliters of a stock solution of pyrene, 4×10^{-3} M in chloroform, was deposited in a 25 mL flask, and after evaporation of the solvent, 8 mL of mesophase was added. To 11 samples of mesophase with pyrene included, small amounts of a 0.1 M stock solution of HDPYCl were added covering a concentration range from 9.1×10^{-4} to 8.2×10^{-3} M. The samples were allowed to equilibrate for at least 48 h at 25 °C, and the fluorescence spectra were recorded with an ISS Greg 200 spectrofluorometer.

Molecular Dynamics. Except for the structures of $TDTMA^+$ and decanol, all bilayer setups, trajectory calculations, and analyses were performed using the software package GROMACS v 3.0.[23] For the visualization of the trajectories and molecular graphics the VMD[24] program was used.

The force field employed was a mixture of GROMOS[26,27] and that of Bergier et al.[28] The bonded part of the potential, namely, bond stretchings, angle bendings, torsions, and out of plane bendings, was obtained from the GROMOS force field, and the nonbonded Lennard-Jones potential was evaluated using the parameters of Bergier et al., since they were developed for aliphatic chains. The united atom approximation was used for the hydrogen atoms in the aliphatic chains. The charges of the different groups in $TDTMA^+$ and DeOH were obtained from 6-31G* ab initio full geometry optimization calculations. The charges of $TDTMA^+$ and DeOH are listed in Table 1. The Ryckaert−Belleman[29] potential function was employed to calculate the potential of the chain torsions. LINCS[30] was used to constrain the bond lengths of the surfactant chains, and SETTLE[31] was used to restrict the structure of the water molecules. A 1 nm cutoff was used for the Lennard-Jones potential and the real space of electrostatic interactions. Long-range electrostatic interactions were calculated using PME.[32,33] The update of the neighbor list was performed every 10 time steps. To maintain the temperature and pressure at constant values of 300 K (water, salt, and surfactant separately), and 1 bar, respectively, we used the Berendsen weak coupling algorithm,[34] with time constants of 0.1 and 1 ps. The time step size in all simulations was 2 fs.

Table 1. Charges of $TDTMA^+$ and DeOH Employed in the Simulations[a]

$TDTMA^+$		DeOH	
$-CH_3$	0.38	H	0.44
$-CH_3$	0.38	O	−0.74
$-CH_3$	0.38	C_1	0.30
N	−0.58	C_2	0.00
C_1	0.31	C_3	0.00
C_2	0.13	C_4	0.00
C_3	0.00	C_5	0.00
C_4	0.00	C_6	0.00
C_5	0.00	C_7	0.00
C_6	0.00	C_8	0.00
C_7	0.00	C_9	0.00
C_8	0.00	C_{10}	0.00
C_9	0.00		
C_{10}	0.00		
C_{11}	0.00		
C_{12}	0.00		
C_{13}	0.00		
C_{14}	0.00		

[a] These values were obtained from a full geometry 6-31G* energy minimization and they are in units of $|e|$.

(17) (a) Leach, A. *Molecular Modelling. Principles and Applications*; Addison-Wesley Longman Ltd: Reading, MA, 1996. (b) Allen, M. P.; Tildesley, D. J. *Computer Simulation of Liquids*; Oxford Science Publications: Oxford, 1987.

(18) Sepúlveda, L.; Cabrera, W.; Gamboa, C.; Meyer, M. *J. Colloid Interface Sci.* **1986**, *117*, 460−463.

(19) Evans, H. C. *J. Chem. Soc.* **1956**, part1, 579−586.

(20) Van Stam, J.; Depaemelaere, S.; De Schryver, F. C. *J. Chem. Educ.* **1998**, *75*, 93−98.

(21) Weiss-Lopez, B. E.; Saldaño, D.; Araya-Maturana, R.; Gamboa, C. *Langmuir* **1997**, *13*, 7265−7269.

(22) Stegemeyer, H. *Lyotrope Flussigkristalle*; Steinkopff Verlag: Darmstadt, 1999; p 45.

(23) van der Spoel, D.; van Buuren, A. R.; Apol, E.; Meulenhoff; P. J.; Tieleman, D. P.; Sijbers, A. L. T. M.; Hess, B.; Feenstra, K. A.; Lindahl, E.; van Drunen, R.; Berendsen, H. J. C. *Gromacs User manual* V *3.0*; Department of Biophysical Chemistry, University of Groningen: Groningen, The Netherlands, 2001.

(24) Humphrey, W.; Dalke, A.; Schulten, K. *J. Mol. Graph.* **1996**, *14*, 33−38.

(25) Berendsen, H. J. C.; Postma, J. P. M.; Gunsteren, W. F.; Hermans, J. Interaction Models for Water in Relation to Protein Hydration. In *Intermolecular Forces*; Pullman, B., Ed.; Reidel: Dordrecht, The Netherlands, 1981; pp 331−342.

(26) Van Gunsteren, W. F.; Berendsen, H. J. C. *Gromos Software Package*; Biomos: Nijenborgh 4, 9747AG, Groningen, The Netherlands.

(27) Van Gunsteren, W. F.; Berendsen, H. J. C. *Angew. Chem., Int. Ed. Engl.* **1990**, *29*, 992−1023.

(28) Bergier, O.; Edholm, O.; Jhaning, F. *Biophys. J.* **1997**, *72*, 2002−2013.

(29) Ryckaert, J. P.; Bellemans, A. *Faraday Discuss. Chem. Soc.* **1978**, *66*, 95−106.

(30) Hess, B.; Bekker, H.; Berendsen, H. J. C.; Fraaije, J. *J. Comput. Chem.* **1997**, *18*, 1463−1472.

(31) Miyamoto, S.; Kollman, P. A. *J. Comput. Chem.* **1992**, *13*, 952−962.

(32) Darden, T.; York, D.; Pedersen, L. *J. Chem. Phys*, **1993**, *98*, 10089−10092.

(33) Essmann, U.; Perera, L.; Berkowitz, M. L.; Darden, T.; Lee, H.; Pedersen, L. G. *J. Chem. Phys.* **1995**, *103*, 8577−8592.

(34) Berendsen, H. J. C.; Postma, J. P. M.; van Gunsteren, W. F.; Dinola, A.; Haak, J. R. *J. Chem Phys.* **1984**, *81*, 3684−3690.

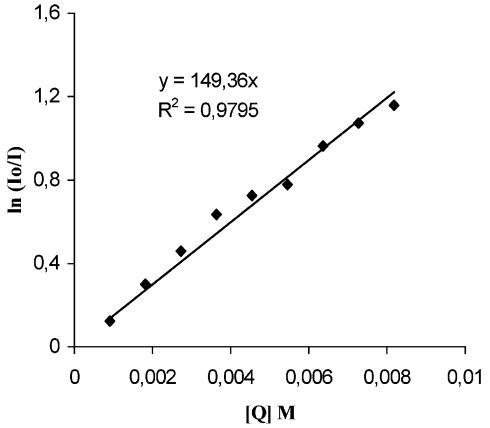

Figure 1. Plot of $\ln(I_0/I)$ vs concentration of quencher.

Results and Discussion

Fluorescence Quenching. The intensity ratio between the vibronic fluorescence bands I ($\lambda = 373$ nm) and III ($\lambda = 384$ nm) of pyrene was employed to test for the location of the probe. The measured $I_I/I_{III} = 1.32 \pm 0.02$ indicates that the probe is probably located at the interface, with a medium polarity close to that of methanol.[35] It also suggests that the integrity of the mesophase remains is stable in all samples. A modification of the mesophase structure that involves modifications in the polarity of the medium should modify the I/III intensity ratio. It has been reported that HDPYCl is completely incorporated to a TDTMABr liquid crystalline bilayer, with the aliphatic chain oriented toward the interior of the bicelle and the aromatic ring near the interface.[36]

The basis of the method assumes a Poisson distribution of the quencher (HDPYCl) inside the aggregates.[16] All pyrene molecules must be associated with an aggregate. Each aggregate can include a maximum of one of each molecule, and emission must arise only from pyrenes in the absence of quencher. In this situation, the intensity ratio in the presence and absence of quencher, I/I_0, becomes

$$I/I_0 = \exp(-[Q]/[M]) \quad (1)$$

where [Q] is the HDPYCl molar concentration and [M] is the concentration of micelles, which can be calculated from

$$[M] = \{[S] - \mathrm{cmc}\}/n \quad (2)$$

[S] is the total molar concentration of surfactant molecules, [TDTMAC] + [DeOH], and cmc is the concentration of free amphiphile. We did not measure the concentration of free detergent in the system, but we used conductivity measurements to determine the cmc of TDTMACl in water, obtaining a value of 0.006 M. Since [S] is 1.73 M, we have neglected the contribution of the nonmicellar detergent to eq 2. With this assumption, it follows from eqs 1 and 2

$$\ln(I_0/I) = [Q]n/[S] \quad (3)$$

Using the height of the first vibronic band ($\lambda = 373$ nm) as a spectral intensity criterion, a plot of $\ln(I_0/I)$ vs [Q] was made and is shown in Figure 1. The slope of this plot multiplied by [S] equals 258 ± 25, the aggregation number, n, which is the number of TDTMACl and decanol units in one micelle. Here the error corresponds to all sources of error, including random experimental errors. This result seems reasonable when compared with the range of values reported for the cesium pentadecafluorooctanoate/water system as a function of temperature, going from about 230 to 270, measured by NMR.[14]

Molecular Dynamics. A unit cell containing two tetradecyltrimethylammonium ions and one central decanol, both with the aliphatic chain in the fully extended 6-31G* minimum energy conformation, was built. The unit cell was copied 8 times in the X direction and 24 times in the Y direction. The generated monolayer, containing 384 $TDTMA^+$ ions and 192 DeOH, was displaced 1.7 nm in the Z direction, copied, and rotated 180° around the Y-axis to generate the desired bilayer. This system was placed in a rectangular box of dimensions $17.2 \times 17.2 \times 6.1$ nm^3, with periodic boundary conditions in all directions, containing 40589 SPC[25] water molecules, 1152 Na^+, and 1920 Cl^- ions. The energy of this bilayer was minimized, to avoid bad contacts and overlaps, and the dynamics run for 12.5 ns. Within the first 250 ps of simulation, the edges of the aggregate, initially with the hydrophobic chains exposed to the water, spontaneously closed to form a continuous curved surface with the polar headgroups pointing toward the solvent. After about 2 ns of trajectory, the system started to show clear signs of spontaneous fractionation and evolved into four or five aggregates with approximately oblate symmetry and similar size. This process was accompanied by a continuous decrease in the potential energy. A closer inspection of the different components of the potential energy reveals that the main contribution to the observed decrease arises from short-range Lennard-Jones and electrostatic interactions of the type ammonium−ammonium, ammonium−solvent, and decanol−solvent. This seems reasonable considering that the fractionation process increases the surface of contact between the headgroups and the solvent and also increases the distance between the positive ammonium headgroups. To estimate a theoretical aggregation number and obtain a more detailed description of the structure of the aggregate, we built three smaller units: (A) 84 TDTMACl, 42 DeOH, 132 NaCl, 4368 H_2O; (B) 160 TDTMACl, 80 DeOH, 252 NaCl, 8320 H_2O; (C) 320 TDTMACl, 160 DeOH, 503 NaCl, 16640 H_2O. The box dimensions were $5.9 \times 6.1 \times 5.6$ nm^3, $7.6 \times 8.2 \times 6.2$ nm^3, and $12.7 \times 12.2 \times 6.8$ nm^3 for systems A, B, and C, respectively. The aggregates were positioned at the center of the box, and periodic boundary conditions were imposed in all directions of space. The mole ratio of all components was maintained constant in all three systems. For systems A and B, 10 ns trajectories were calculated and all the analysis performed on the last 6 ns. For system C, only 5 ns of simulation was calculated for reasons explained below. Figure 2 shows two perspectives of systems A and B after 9 ns and system C after 5 ns trajectory. To check for the stability of the different aggregates, the calculated potential energy was examined. Since all systems have the same mole fraction for all components, to make the values comparable we divided the potential energy by the number of TDTMACl units. The result, $E_{(A)} = -3869.1$ kJ, $E_{(B)} = -3995.6$ kJ, and $E_{(C)} = -3996.9$ kJ, indicates that aggregates B and C should be the most stable. The energy differences observed between (B) and (C) do not allow an unequivocal conclusion of which one should be preferred. Reliable energy differences of the order of 1 kJ between these large systems are not yet possible to obtain by classical mechanics simulation. It is very likely that the real sample is composed of a distribution of aggregate sizes, very close in energy. After 250 ps of simulation, the

(35) Kalyanasundaram, K.; Thomas, J. K. *J. Am. Chem. Soc.* **1977**, *99*, 2039−2044.
(36) Weiss-Lopez, B. E.; Gamboa, C.; Tracey, A. S. *Langmuir* **1995**, *11*, 4844−4847.

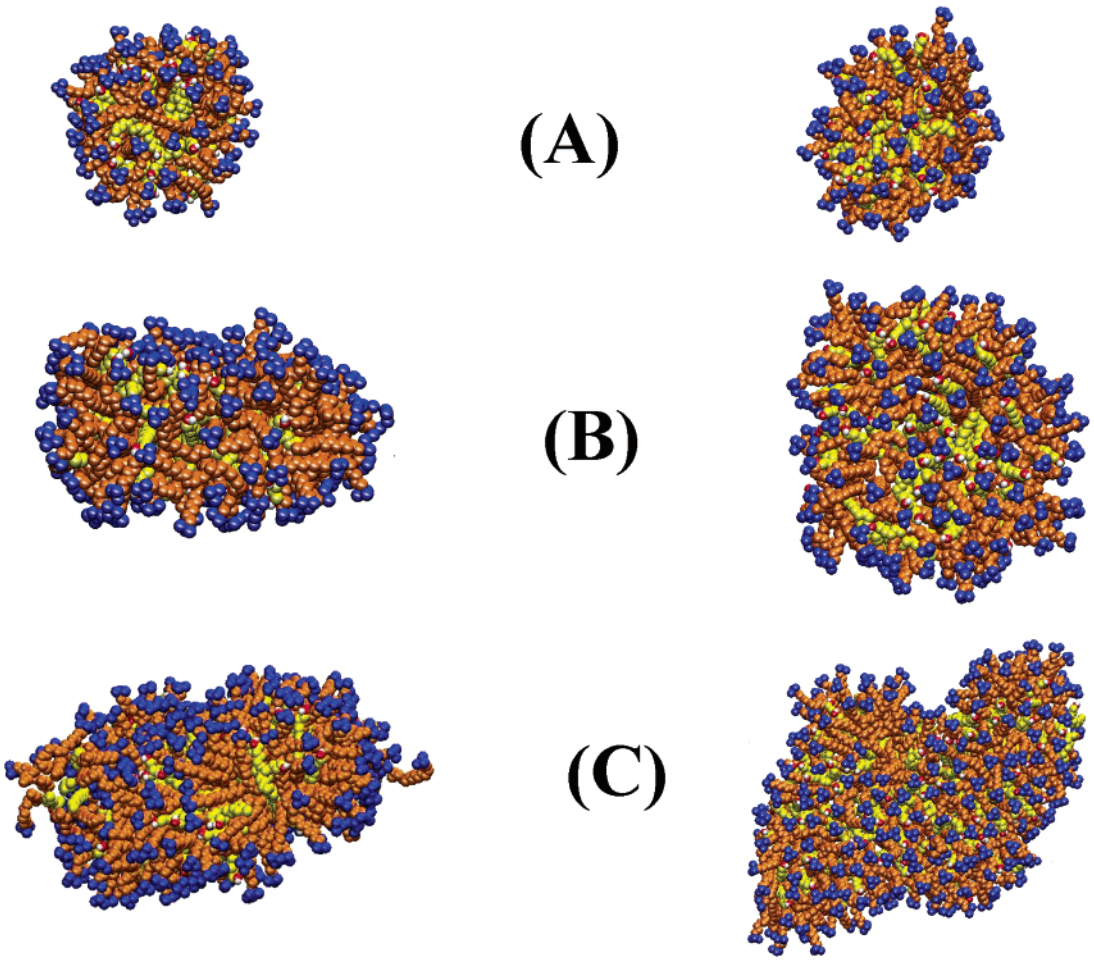

Figure 2. Snapshots of systems A (10 ns), B (10 ns), and C (5 ns) from different perspectives. On the left there is a view along the *Y* axis of the box and on the right a view along the *Z* axis of the box. The methylammonium headgroups are blue and the hydrocarbon tail is orange; oxygen atoms of DeOH are red, H atoms of DeOH are white, and the chain is yellow.

solvent exposed edges in aggregate A closed and a structure closer to a spherical micelle rather than to a bilayer evolved. Aggregate B, with similar initial configuration and solvent exposed edges, quickly evolved into an oblate average symmetry, closing the edges and forming a continuous curved surface. After 2 ns of simulation, system C showed clear signs of deformation, similar to that observed in the fractionation of the large bilayer, although no division was observed up to 5 ns. This calculation was stopped at this point, and aggregate C was discarded for further analysis. Figure 3 shows the radii of gyration, R_gX, R_gY, and R_gZ, along the principal axes of aggregates A and B, as a function of time. System A evolves to a structure with the three radii of gyration approximately equal, characteristic of a spherical shape. Structure B evolves to an average oblate symmetry, with $R_gZ > R_gX \cong R_gY$, and remains more or less unchanged during the complete simulation. System C displays three different time dependent radii of gyration, evidence of the continuous deformation and lack of symmetry of the aggregate. As inferred from the behavior of the radii of gyration, aggregate B did not experience significant variations in shape during the simulation. Visual inspection of the trajectory reveals that the orientation of the aggregate, with reference to the box axis, remained practically unchanged during the simulation, with the symmetry axis of the oblate along the *Z*-axis of the box. The observed stability throughout the dynamics, and the nice anisotropic distribution of surfactants in system B, suggest that the system is at equilibrium. This is a reasonable representative model of the aggregate from which statistical properties could be obtained with some confidence. It is composed of 240 surfactant molecules, 160 TDTMACl and 80 DeOH, in excellent agreement with the fluorescence experimental determination, 258 ± 25, and previous measurements in other similar aggregates.[14] Figure 4 shows the potential energy of (B) as a function of time. The fluctuation is about 0.5% of the total energy. Therefore, we have employed system B to make a more complete characterization of the

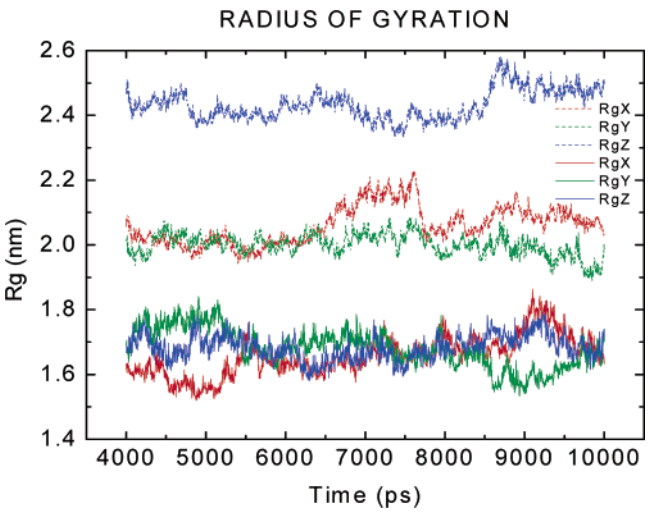

Figure 3. Radius of gyration along the principal axis of aggregates A (solid lines) and B (dashed lines).

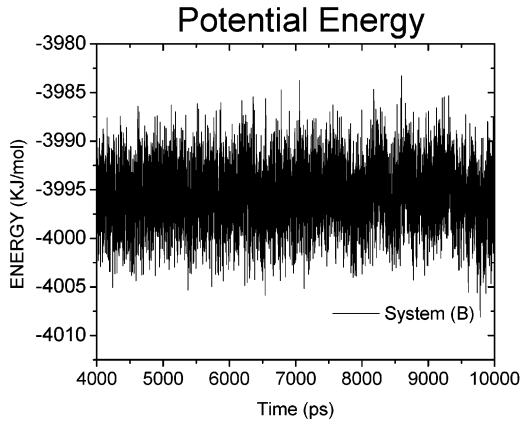

Figure 4. Potential energy of system B as a function of time.

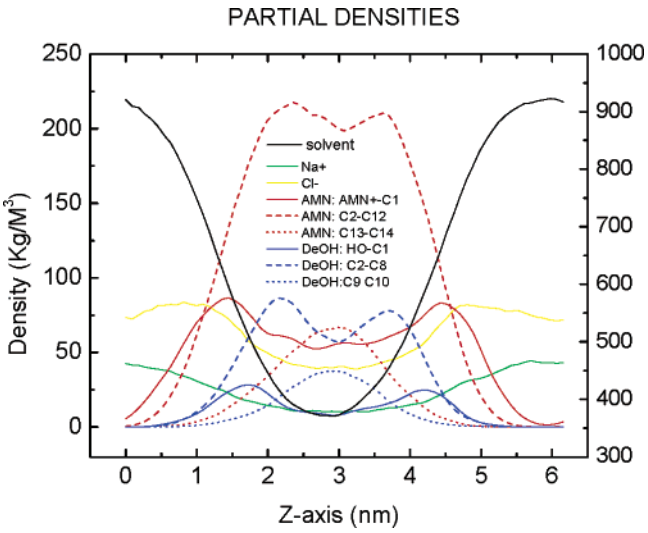

Figure 5. Density profile of all components of aggregate B, along the *Z* axis of the box. The big scale on the right applies to the solvent; the smaller scale on the left applies to the other components.

liquid crystal unit and the detailed analyses below were performed on this system only.

Figure 5 shows the mass density profile of the solvent and all the other components of the liquid crystal along the normal to the surface of the micelle, the *Z*-axis of the box. Because the aggregate was placed at the center of the box, it remains completely surrounded by solvent and ions during the complete trajectory. This has the effect that the calculated densities, along the normal of the aggregate's surface, never decrease to zero. However, it is still possible to estimate the distribution and orientation of the different components of the bilayer.

Using a previous definition of interfacial width,[37] in this case the region where the density of H_2O decreased from 10% of the total range below its maximum (865 kg/m^3) to 10% of the total range above its minimum (425 kg/m^3), the thickness of the interface was estimated to be about 1.7 nm. The thickness of the hydrophobic core can be estimated to be 1.4 nm. To study the orientation and distribution of the surfactant molecules, $TDTMA^+$ and DeOH, in the aggregate, their structures were divided into three parts: (1) the headgroup including the first methylene carbon, (2) the central hydrophobic region, and (3) the last two carbons of the chain. Figure 5 clearly shows that $TDTMA^+$ as well as DeOH constitutes the bilayer,

(37) Tieleman, D. P.; van der Spoel, D.; Berendsen, H. J. C. *J. Phys. Chem. B* **2000**, *104*, 6380−6388.

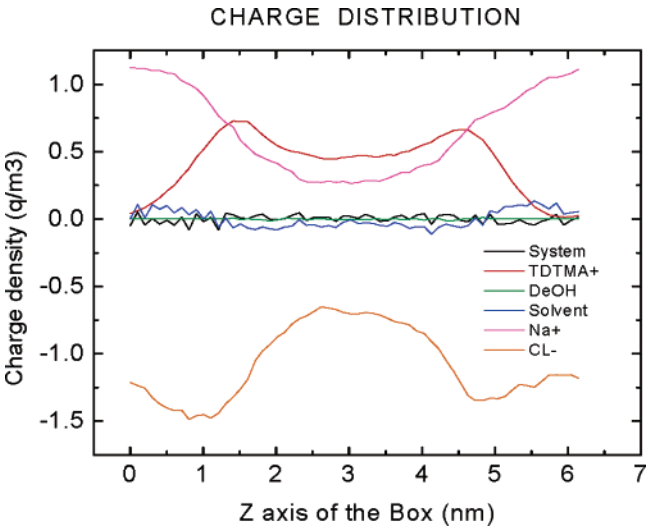

Figure 6. Distribution of charges along the *Z* axis of the box.

with the headgroups exposed to the solvent and the hydrophobic chain to the interior. However the DeOH headgroup is located, on average, about 0.3 nm more to the interior of the aggregate, contributing to widening the interface possibly by attracting water molecules to the OH group. The hydrogen bond distance distribution between the oxygen of DeOH and protons from water was calculated and shows the existence of a preferential O···H distance of 0.17 nm, possibly due to the existence of a H bond. The radial distribution function of the $TDTMA^+$ headgroup with the solvent was calculated. An estimate of the cumulative number, considering up to the first maximum in the radial distribution function, indicates that there are 16 solvent molecules in the first solvation shell of the ammonium headgroup.

Figure 5 also shows that the density of the sodium ions decreases when approaching the region where the ammonium headgroups are located, and the density of chloride ions increases when approaching the same region, as expected from basic electrostatics.

Figure 6 plots the total charge density as well as some of its components as a function of the *Z*-axis of the box. It clearly shows a strong polarization of the chloride ions at the interface due to the ammonium headgroups. The distance from the maximum charge density of the ammonium headgroups to the point where the polarization of the Cl^- ions disappears is about 1.1 nm.

The mobility of the two components of the bilayer in the *XY* plane was also examined. In 6 ns of trajectory, the components of the aggregate, $TDTMA^+$ and DEOH, displace about 2.5 nm in the *XY* plane. There is a random distribution of DeOH and $TDTMA^+$ in the *XY* plane after equilibration.

The interior of the aggregate was examined by calculating the diagonal elements of the order parameters tensor of both constituents of the micelle along the aliphatic chain, relative to the *Z* axis of the box. Since the hydrogen atoms of the chains are not represented explicitly, their positions are reconstructed based on the positions of the carbon atoms along the chain.[37] The order parameters for the last carbon of the tail cannot be calculated. Figure 7 shows the diagonal elements of the order parameter tensor for $TDTMA^+$ and DeOH. As expected, $|S_{xx}|$ and $|S_{yy}|$ are smaller than $|S_{zz}|$ since there is more rotational space available for the methylene in the *XY* plane, in both cases. It is observed for $TDTMA^+$ that the first two methylene groups show the highest degree of order, followed by a long segment, from C4 to

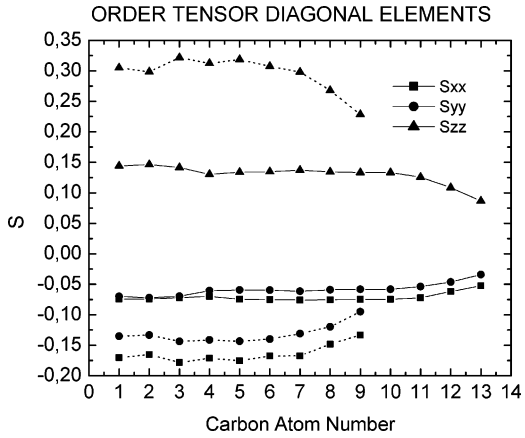

Figure 7. Order parameters of the aliphatic chains of $TDTMA^+$ and DeOH. The dotted line corresponds to DeOH, and the continuous line is $TDTMA^+$.

C10, with slightly less but constant order, to finally decrease the order progressively in the last carbons of the tail. For DeOH, C1 and C2 carbons are less ordered than those from C3 to C7; the last two carbons are even less ordered. The reduced order for C1 and C2 might arise from the dynamics of the H-bond with the solvent. The system seems to have a high degree of order, only slightly less than, e.g., phosphatidylcholine lipids in the liquid crystalline state.[38]

Conclusions

The aggregation number of a four-component lyotropic liquid crystal has been examined for the first time using two methodologies: fluorescence quenching and molecular dynamics simulations. The fluorescence experiments give an average aggregation number of the studied liquid crystal of 258 ± 25 units. This is in good agreement with previous determinations in similar systems.[14] MD simulations suggest a stable aggregate of 240 units, in agreement with the fluorescence measurement. A lower limit greater than 126 units to form the discotic aggregate is predicted by the MD simulation. An aggregate with that number of units becomes a spherical micelle, and no anisotropy should be detected. According to the MD results, the existence of larger aggregates is possible, although their shapes are not well-defined. This could explain the nonregular structure of some aggregates detected by NMR diffusion experiments.[9] The real sample probably consists of a distribution of aggregate with different sizes and similar energy. After equilibration, the components of the aggregate are randomly distributed in the micelle and no cluster formation of DeOH or $TDTMA^+$ was observed.

Finally, the simulation locates the DeOH headgroup, on average, 0.3 nm more to the interior of the bilayer than the ammonium headgroups, forming H-bond with the solvent and possibly widens the interface.

Acknowledgment. The authors are pleased to acknowledge financial assistance from Fondecyt, Grants Nos. 1010211 and 7010211. H.A. and R.M. acknowledge Doctoral Fellowships from Conicyt. D.P.T. is a Scholar of the Alberta Heritage Foundation for Medical Research.

Supporting Information Available: Textures of the TDTMACl mesophase observed using polarized light microscopy (Figure SI 1), series of fluorescence spectra of pyrene at different concentrations of quencher (Figure SI 2), a snapshot of the large system after 12.5 ns trajectory showing clear signs of fractionation into four or five smaller units (Figure SI 3), distance distribution between the oxygen from decanol and protons from the solvent of system B (Figure SI 4), radial distribution function $TDTMA^+$–solvent of system B (Figure SI 5), cumulative number as a function of radius (Figure SI 6), trajectories of $TDTMA^+$ and DeOH headgroups in the *XY* plane in 6 ns of system B (Figure SI 7). This material is available free of charge via the Internet at http://pubs.acs.org.

(38) Tieleman, D. P.; Marrink, S. J.; Berendsen, H. J. C. *Biochim. Biophys. Acta* **1997**, *1331*, 235−270.